Effect of spatially asymmetric dipolar interactions in the magnetization reversal of closely spaced ferromagnetic nanoisland arrays

J. M. Porro, A. Berger, M. Grimsditch, V. Metlushko, B. Ilic et al.

Citation: J. Appl. Phys. **111**, 07B913 (2012); doi: 10.1063/1.3677269
View online: http://dx.doi.org/10.1063/1.3677269
View Table of Contents: http://jap.aip.org/resource/1/JAPIAU/v111/i7
Published by the American Institute of Physics.

Additional information on J. Appl. Phys.

Journal Homepage: http://jap.aip.org/
Journal Information: http://jap.aip.org/about/about_the_journal
Top downloads: http://jap.aip.org/features/most_downloaded
Information for Authors: http://jap.aip.org/authors

ADVERTISEMENT

Downloaded 16 May 2013 to 158.227.184.199. This article is copyrighted as indicated in the abstract. Reuse of AIP content is subject to the terms at: http://jap.aip.org/about/rights_and_permissions

Effect of spatially asymmetric dipolar interactions in the magnetization reversal of closely spaced ferromagnetic nanoisland arrays

J. M. Porro,[1,a)] A. Berger,[1] M. Grimsditch,[1,2,3] V. Metlushko,[4] B. Ilic,[5] and P. Vavassori[1,2]
[1]*CIC nanoGUNE Consolider, 20018 Donostia-San Sebastián, Spain*
[2]*IKERBASQUE, Basque Foundation for Science, 48011 Bilbao, Spain*
[3]*Materials Science Division, Argonne National Laboratory, Argonne, Illinois 60439, USA*
[4]*Department of Electrical and Computer Engineering, University of Illinois at Chicago, Chicago, Illinois 60607, USA*
[5]*Cornell Nanofabrication Facility, Cornell University, Ithaca, New York 14853, USA*

(Presented 2 November 2011; received 23 September 2011; accepted 14 November 2011; published online 7 March 2012)

The magnetization reversal process of interacting elongated nanoislands is presented here. The magnetization reversal has been investigated by means of magneto-optical Kerr effect magnetometry, analyzing the beams reflected and diffracted by the array, magnetic force microscopy, and micromagnetic simulations. The nanoislands have an aspect ratio of 4.2 and are arranged in chiral square units forming a checkerboard array. Due to this particular arrangement, each island is subjected to a spatially asymmetric dipolar interaction field. We found that for certain directions of the applied field this specific character of the dipolar interaction affects the reversal process profoundly. In these cases the magnetization reversal takes places via the nucleation and displacement of a vortex state in two of the four nanoislands in every square unit, at variance with single domain rotation process generally observed for other directions of the applied field. © *2012 American Institute of Physics*. [doi:10.1063/1.3677269]

Understanding and controlling the effects of dipolar interactions between ferromagnetic nanoelements is crucial for many technical applications of magnetism such as ultra-high density memories for hard disk storage, magnetic random access memories, and magnetic quantum-dot cellular automata systems for digital computations.[1] From a fundamental point of view, dipolar interactions among ferromagnetic nanoelements can be exploited to study the fundamental physical phenomenon of frustration, as in the case of artificial spin-ice systems,[2] where the magnetic moment orientation of the nearest neighbor nanoelement follows a rule analogous to that of atomic spins located in each vertex of a tetrahedral, the so-called 2-in/2-out spin-ice rule. The utilization of nanomagnets for such fundamental studies relies on a nanoelement design resulting in an Ising-like behavior, i.e., each nanomagnet must have a bistable single-domain configuration, which is usually facilitated by means of shape anisotropy. By increasing the aspect ratio of the nanoelements under the action of an external field each nanoelement flips between two single domain magnetic configurations pointing in opposite directions along the long axis of the nanoelement. For thin submicron noninteracting elliptical nanoelements made of soft ferromagnetic materials, such as Permalloy, using dimensions of 30 nm thickness and 200 nm width, this behavior is ensured for aspect ratios higher than 3.[3] Moreover, it is crucial that the Ising-like behavior is preserved when the nanoelements are interacting through their dipolar stray fields. In this study we address the relevant case of high aspect ratio nanomagnets whose geometric arrangement leads to spatially inhomogeneous and asymmetric dipolar magnetostatic field coupling. The nanomagnets are bars made of Py, 720 nm long, 170 nm wide, and 25 nm thick corresponding to an in-plane aspect ratio of 4.2. They are organized on a checkerboard array of square units, with each square unit being formed by four nanoelements arranged in a chiral structure.

The array of nanomagnets has been fabricated by means of patterning using electron beam lithography and lift-off processes combined with electron beam evaporation for the deposition of Py. The gaps between neighboring nanoislands are 100 nm. The square unit separation (corner to corner) is 200 nm so that dipolar interactions between nanomagnets belonging to different units are clearly weaker so that they do not affect the magnetization reversal process. The lateral period of the array, along both the vertical and horizontal direction, is 2.2 μm. The magnetization reversal process has been investigated experimentally using magneto-optic Kerr effect (MOKE) magnetometry and magnetic force microscopy (MFM), and modeled using micromagnetic simulations. MOKE magnetometry measurements have been carried in the conventional longitudinal-MOKE (L-MOKE) configuration[4] from the beam reflected by the sample as well as in the so-called diffracted-MOKE (D-MOKE) geometry[5] using the beams diffracted by the array. In D-MOKE, one typically records the transverse MOKE effect using "*p*" polarization and having H perpendicular to the scattering plane. As shown in Ref. 5, the field dependent intensity measure in D-MOKE is proportional to $f_n(H) = \int m_y(r,H) \cdot \exp(inG_x x)dS$ where n is the diffraction order, $m_y(r,H)$ is the vertical component of the magnetization spatial distribution in the magnetic material and $G_x=2\pi/L_x$, with L_x being the lateral distance between neighboring square units in the array. Using micromagnetic simulations $m_y(r,H)$ can be

a)Electronic mail: t.porro@nanogune.eu.

 © 2012 American Institute of Physics

Downloaded 16 May 2013 to 158.227.184.199. This article is copyrighted as indicated in the abstract. Reuse of AIP content is subject to the terms at: http://jap.aip.org/about/rights_and_permissions

computed and the D-MOKE loop of any order n, including the reflected beam loops corresponding to $n=0$, can be obtained by calculating f_n. The side-by-side comparison of the simulated and experimental D-MOKE loops permits to confirm the validity of the micromagnetic configurations provided by the simulations or, if required, to revise the assumptions in the simulations (shape details, material parameters) until agreement is achieved. The combination of D-MOKE and micromagnetic simulations constitutes a powerful tool to study the spatial correlation of magnetization at the nanoscale thanks to the extreme sensitivity of the D-MOKE hysteresis loops to the details of the magnetization distribution in the array unit cell.[6] Micromagnetic simulations were performed utilizing the object oriented micromagnetic framework (OOMMF) platform provided by NIST.[7] The material parameters used for the simulations are those contained in the OOMMF program for Permalloy (saturation magnetization $Ms=860\times10^3$ A/m, exchange stiffness constant $A=13\times10^{-12}$ J/m^3, no magnetic anisotropy, and a damping coefficient of 0.5). To keep the computational time reasonable, we used a cell size of 10 nm, which is bigger than the exchange length in Permalloy that is 5.4 nm for the material parameters used in the simulations. We verified that the use of this rather large unit cell size does not affect the results of simulations by calculating a few selected configurations with a cell size of 5 nm. Magnetic force microscopy (MFM) was used to image the remanent magnetic configurations in the nanoelements. The tool used to perform magnetic force imaging is an Agilent® 5500 Atomic Force Microscope, with a magnetically coated (CoCr) tip. We measured L- and D-MOKE loops for different orientations of the external applied field. Figure 1 shows the hysteresis loops measured on the array of nanoelements for two different orientations of the applied field H, namely at an angle larger and smaller than 1.5° away from the edge orientation of a nanoelement, referred to as "misaligned" and "aligned" cases hereafter. Although we have measured D-MOKE from several diffracted orders, we show and discuss here only the second order loops since they were the most sensitive to the details of the magnetization reversal. In the representative loops for the misaligned and aligned cases, shown in Fig. 1, H was applied at 2.5° and 0.5° away from the unit cell edge orientation.

Both the L-MOKE and D-MOKE hysteresis loops show that the magnetization reversal process in the array undergoes a substantial change upon changing the field orientation from the misaligned to the aligned case. These differences are particularly apparent in the second-order diffracted beam hysteresis loops. Therefore, we will focus our discussion primarily on the D-MOKE loops. The corresponding D-MOKE loops for the second-order diffracted beam are shown in Fig. 2. The agreement between the experimental and calculated loops is remarkable, as all the features of the experimental loops are reproduced in great details by the calculated ones. The H values at which the various features appear are slightly different in the simulations. This is not surprising considering that the simulations are performed using particles having a perfect shape and at $T=0$ K. Having established the reliability of the micromagnetic simulations by its excellent correspondence to our experimental observations, we can use the computed magnetization configurations to analyze the magnetization reversal of each nanoelement in detail. The relevant micromagnetic configurations computed for the two cases, aligned and misaligned, are shown in Fig. 3. As can be seen, starting from positive saturation ($H=2.3$ kOe) where the configuration is substantially the same for both cases, the magnetization reversal follows two completely different routes after reducing the field (compare configuration B and B′ in Fig. 3 at $H=1.3$ kOe). In the misaligned case, we observe the formation of a "S" state in the horizontal islands (configuration B). As the field is further reduced, the "S" state rotates according to configurations C, D, E, and F. As a result, all elements in the square unit remain in a nearly uniform, single domain state during the complete reversal process, hereby giving rise to a sequence of configurations for the entire square unit cell that resembles the so called "onion state" (configuration C), "horse-shoe state" (configuration D), and "reversed onion state" (configuration E) observed in closed square ring structures.[8] The formation of the horse-shoe state is due to the fact that the nanoelements are not perfectly identical so that the two vertical structures switch at

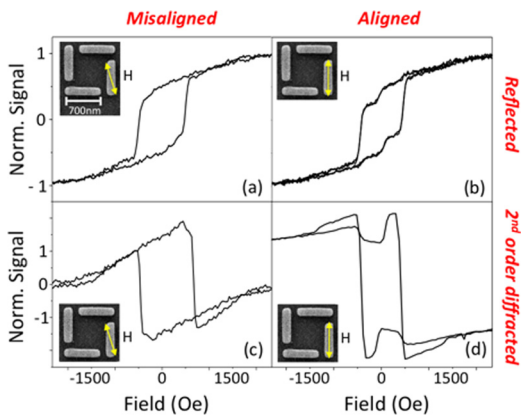

FIG. 1. (Color online) Measured hysteresis loops from the reflected (a, b) and second order diffracted (c, d) beams in the misaligned (a, c) and aligned (b, d) cases, with insets showing a SEM image of the unit square and the direction of the applied field.

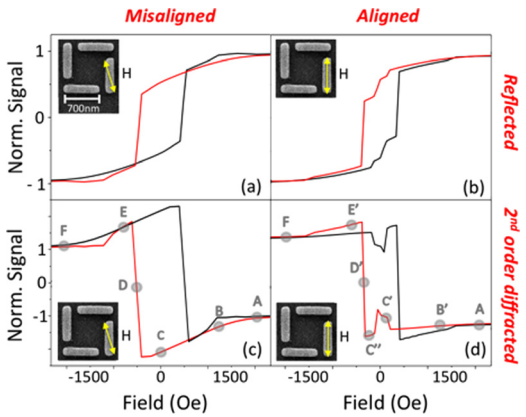

FIG. 2. (Color online) Calculated hysteresis loops from the reflected (a, b) and second order diffracted (c, d) beams in the misaligned (a, c) and aligned (b, d) cases, with insets showing a SEM image of the unit square and the direction of the applied field. The positions marked in the diffracted hysteresis loops correspond to the magnetization states shown in Fig. 3.

Downloaded 16 May 2013 to 158.227.184.199. This article is copyrighted as indicated in the abstract. Reuse of AIP content is subject to the terms at: http://jap.aip.org/about/rights_and_permissions

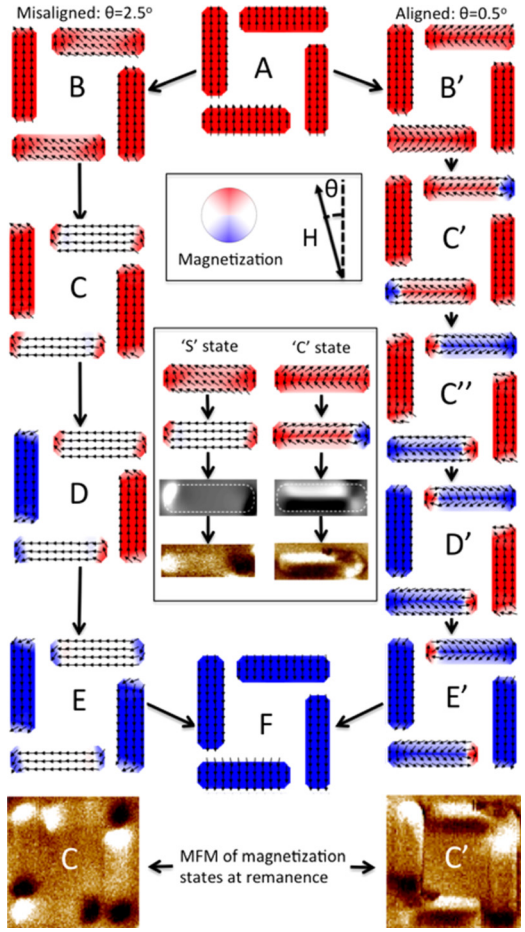

FIG. 3. (Color online) Micromagnetic simulations of the magnetization states in the magnetization reversal process for the misaligned and aligned cases corresponding to the marked points in the hysteresis loops of Fig. 2. Inset 1: Sketches indicating the external field and the magnetization directions. Inset 2: differences in the magnetic states of the horizontal bars for the misaligned and aligned cases. The sequence shows the seed "S" (misaligned) and "C" (aligned) magnetic states, followed by their corresponding remanent states, the calculated MFM image of these magnetic states, and the obtained MFM image showing a single-domain (misaligned) and a vortex (aligned) magnetic states. Lower inset: MFM images obtained at remanence for the misaligned (C) and aligned cases (C′).

slightly different field values. These findings demonstrate that dipolar interactions are not relevant enough to cause a deviation from the anticipated single domain rotation process in this case and the reversal is governed by the shape anisotropy of the individual nanoelements.

A completely different picture emerges in the aligned case. In this case the different loop shape reveals that dipolar interactions are able to overcome the effect of the shape anisotropy and induce a "C" state into each of the individual horizontal elements (configuration B′) rather than a "S" state as the external field is reduced from positive saturation. The "C" state subsequently nucleates a single vortex in each horizontal nanoelement as H is reduced to zero (configuration C′). Interestingly, in the remanent configuration the two vortices are distorted with their cores displaced in order to reduce the magnetostatic energy due to the stray field produced by the vertical nanoelements. As the external field reverses, the vortex cores are displaced horizontally towards the opposite end of each horizontal nanoelement (configuration C"). The vortex cores displacements produce the notable peaks in the 2nd order D-MOKE loop. This vortex core displacement is a reversible process as we verified relaxing the external field to zero from the value corresponding to the peak positions in the loops and observing that the D-MOKE signal retraces itself. By decreasing the field H past the peak, the two vertical elements switch one at a time (configurations D′ and E′) as in the previous case. At a negative field of −1.4 kOe, the vortices eventually annihilate before reaching saturation. It is worth noticing that the vortices in the horizontal islands have opposite chirality, which is predetermined by the chirality of the square unit structure and the direction of the applied field. Confirmation of the reversal processes described above was obtained using MFM studies of the remanent state in the two cases. The lower inset of Fig. 3 shows the resulting MFM images of the remanent states in the horizontal nanoelements compared to the expected MFM images calculated based on the configurations C and C′ obtained with OOMMF. The MFM images clearly exhibit the magnetization pattern of states C and C′ proposed by our micromagnetic simulations shown in Fig. 3.

In conclusion, we investigated the role of spatially inhomogeneous and asymmetric magnetostatic interactions onto the magnetization reversal of interacting elongated nanoelements arranged in square units with chiral structure. Analysis of the diffracted magneto-optical Kerr effect hysteresis loops, magnetic force microscopy images, and micromagnetic simulations show that the magnetization reversal path depends very sensitively on the in-plane direction of the applied magnetic field. When the external field is applied at an angle bigger than 1.5° away from the edge orientation of the array square units the reversal is dominated by the shape anisotropy of the nanoislands and magnetostatic dipolar interactions do not play a relevant role. When the external field is applied at an angle smaller than 1.5°, magnetostatic interactions modify substantially the magnetization reversal path. The spatial asymmetry of the dipolar interaction field causes the formation of vortex states of well-defined chirality in the nanoelements with their short axis parallel to the applied field.

We acknowledge funding from the Basque Government under Program No. PI2009-17, the Spanish Ministry of Science and Education under Project No. MAT2009-07980 and the Basque Government fellowship No.BFI09.289. V.M. acknowledges funding from U.S. NSF, Grant No. ECCS-0823812.

[1]A. Imre, G. Csaba, L. Ji, A. Orlov, G. H. Bernstein, and W. Porod, Science **311**, 5758 (2006).
[2]R. F. Wang, C. Nisoli, R. S. Freitas, J. Li, W. McConville, B. J. Cooley, M. S. Lund, N. Samarth, C. Leighton, V. H. Crespi, and P. Schiffer, Nature **439**, 303 (2006).
[3]N. A. Usov, C. R. Chang, and Z. H. Wei, J. Appl. Phys. **89**, 7591 (2001).
[4]P. Vavassori, Appl. Phys. Lett. **77**, 1605 (2000).
[5]M. Grimsditch and P. Vavassori, J. Phys: Condens. Matter **16**, R275 (2004).
[6]T. Verduci, C. Rufo A. Berger, V. Metlushko, B. Ilic, and P. Vavassori, Appl. Phys. Lett. **99**, 092501 (2011).
[7]OOMMF code made by NIST: http://math.nist.gov/oommf/.
[8]P. Vavassori, M. Grimsditch, V. Novosad, V. Metlushko, and B. Ilic, Phys. Rev. B **67**, 134429 (2003).

Downloaded 16 May 2013 to 158.227.184.199. This article is copyrighted as indicated in the abstract. Reuse of AIP content is subject to the terms at: http://jap.aip.org/about/rights_and_permissions